Reconfigurable multi-rotor for high-precision physical interaction

Joshua Taylor[1,2], Nursultan Imanberdiyev[2], Meng Yee (Michael) Chuah[2],
Wei-Yun Yau[2], Guillaume Sartoretti[1], and Efe Camci[2]

***Abstract*— Unmanned aerial vehicles (UAVs) for contact-based tasks at height can greatly improve the safety of the human workers involved. However, enabling physical interaction with typical under-actuated UAVs is non-trivial. Due to their coupled translational and rotational dynamics and limited station-keeping performance, it is difficult to maintain precise and consistent contact. We address these problems in the context of physical interaction with vertical, cylindrical target objects, such as trees. We present a novel UAV design with a pair of tilt-rotors and a landing gear that can reconfigure into a front-mounted, two-fingered gripper. This landing gear is implemented as a cable-driven under-actuated system, which requires only one actuator to control both the reconfiguration and the grasping (i.e., five degrees of freedom in total). The tilt-rotors and reconfigurable landing gear enable the UAV to obtain support from the target object during physical interaction tasks. Such support results in more than 80% improvement in position- and heading-keeping performance. We achieve this performance upgrade without a significant increase in the power consumption of the UAV thanks to our lightweight design with minimal actuators. This marks progress towards safe, high-precision physical interaction against vertical, cylindrical target objects.**

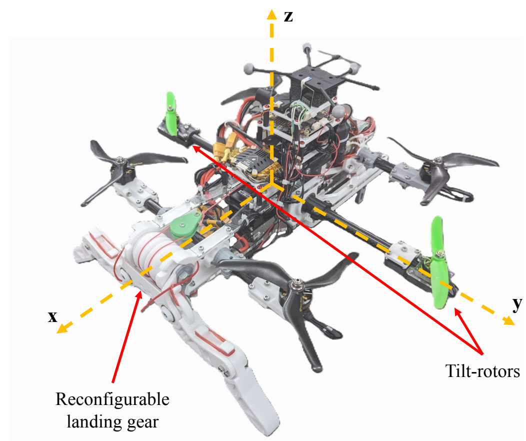

Fig. 1. Novel UAV prototype for high-precision physical interaction.

I. Introduction

Unmanned aerial vehicles (UAVs) are unmatched in their ability to operate in hard-to-reach places at high altitudes. This has resulted in their use across many applications, from search and rescue [1] to nature conservation [2]. Most of these applications involve simple surveillance tasks where the UAV can maintain safe distances from any obstacles. More recently, there has been a drive to reap the benefits of UAVs in applications involving physical interaction with the environment. For example, UAVs have been used for aerial screwing and drilling [3], contact-based inspection of power lines [4], and sensor placement on trees [5]. These tasks are typically conducted by human workers, which often require them to reach dangerous locations. Providing UAVs that can handle these tasks has significant implications for worker safety and the amount of resources required.

However, transitioning from vision-based to contact-based tasks is non-trivial for UAVs [6]–[8]. Many applications require contact to be made at a specific location on the target object, for example, to mate with a previously placed bolt for unscrewing. Furthermore, during physical interaction, deviation from a pose setpoint can lead to high levels of stress on the end effector. These factors present the need for high positional accuracy prior to and during contact. Such accuracy is difficult to achieve due to the under-actuation of typical rotary-wing UAVs, i.e., they have fewer actuators than degrees of freedom (DoFs), and their translational and rotational dynamics are coupled. Furthermore, the wall effect starts to occur while flying very close to a target object and acts as a disturbance. All these make it difficult to precisely control the UAV's pose and accurately maintain contact with external objects.

One approach used in the literature to mitigate these issues is adding further DoFs to the manipulator so that it can move relative to the UAV's body [9], [10]. This alleviates the need for high positional accuracy of the UAV because the manipulator can reach the target location even though the UAV is not perfectly positioned. Alternatively, the manipulator can also be rigidly fixed to the UAV's body when fully-actuated or over-actuated UAVs are used [6]–[8], [11]. Such UAV designs have a number of actuators equal to or greater than the number of DoFs, respectively, which allow them to translate without pitching and rolling, and hover at any arbitrary angle. However, this comes at the cost of additional actuators; therefore, researchers have also explored minimal configurations to obtain only the required benefit. For example, by mounting a single horizontal thruster, the UAV in [12] can generate forward thrust without pitching.

To further improve a UAV's stability during interaction and allow for the generation of larger forces, one can also explore using the target object as support via perching mechanisms. The key challenge here is keeping the design lightweight, hence the adoption of under-actuated cable-driven mechanisms [13], [14], bi-stable mechanisms [15], and reconfigurable UAV bodies [16], which typically al-

[1]National University of Singapore (NUS), Singapore
[2]Institute for Infocomm Research (I^2R), A*STAR, Singapore

Manuscript 538 submitted to 2024 IEEE/RSJ International Conference on Intelligent Robots and Systems (IROS). Received February 29, 2024.

low for fewer added actuators and components. The most common approach for perching on vertical surfaces is using suction-based mechanisms [3], [17], [18]. While this method performs well in urban environments with smooth concrete target surfaces, it does not translate well to rougher surfaces like tree bark. Furthermore, several such perching mechanisms are mounted to under-actuated UAVs and, therefore, require agile maneuvers for landing on vertical or near-vertical surfaces [18]–[20]. This may not be suitable for heavy UAVs with high payloads.

In this manuscript, we present a novel multi-rotor platform for precise contact-based applications against vertical, cylindrical target objects, such as trees and poles. The UAV has a pair of variable tilt-rotors and a landing gear that can reconfigure into a front-mounted gripper. These require the addition of only two actuators to the UAV, resulting in an overall lightweight design. These mechanisms allow the UAV to stabilize itself against the target object. Through real-world experiments involving interaction with a tree-like target, we show that this capability yields significantly improved position and yaw control. This is key in enabling more stable and safer interactions of the UAV with the environment. Importantly, our system is not limited to smooth vertical surfaces and avoids requiring agile maneuvers to make contact. In summary, the key contributions of this work are:

- A novel UAV design with two tilt-rotors and a landing gear that can be reconfigured as a gripper.
- Design of such lightweight and versatile landing gear which requires only one servo motor for actuation.
- Improved position and yaw control during physical interaction for safer high-precision applications against vertical surfaces of cylindrical objects.

The remainder of this manuscript is structured as follows. Section II describes the proposed UAV, Section III discusses its control, and Section IV describes the real-world experiments conducted. Finally, Section V describes the current system's limitations, and Section VI draws the key conclusions.

II. The UAV

The UAV concept is shown in Fig. 1. It has four primary thrust rotors arranged in a 450 mm×450 mm square, and two smaller tilt-rotors which are longitudinally centered and laterally 200 mm apart from the center line. The UAV has a landing gear that can reconfigure into a gripper, henceforth referred to as the *reconfigurable landing gear* (RLG).

A. Tilt-Rotors

To enable the UAV to generate a forward or backward force without pitching, we add a pair of tilt-rotors to the UAV. This acts as an almost minimal configuration to decouple pitch and longitudinal motion. This allows for more controlled and precise movement when approaching the target object and can aid in generating supportive forces for contact-based work, such as a feed-force for drilling. The mechanism used to tilt the rotors is shown in Fig. 2. The two rotors are fixed to one arm, which runs through the center

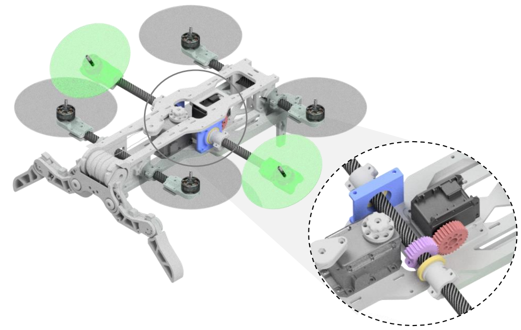

Fig. 2. The tilt-rotor mechanism, consisting of two rotors (green), which rotate simultaneously about the arm's central axis. A gear (red) is fixed to a servo motor head, which drives a gear (purple) on the rotor arm. The arm rotates via bearings (yellow), which fit within a custom housing (blue).

of the UAV body. This arm is rotated via a 1:1 gear train powered by an off-axis servo motor. Rotation of the arm allows for simultaneous tilting of the rotors about the UAV's y-axis.

B. Reconfigurable Landing Gear

The key novelty of the UAV is the RLG, which can be raised for use as a gripper, as shown in Fig. 3. This enables grasping onto the target object such that the UAV can rigidly fix itself in place, allowing for the opposition of a wider range of forces during interaction. Therefore, the RLG can provide improved station-keeping performance and facilitate applications with greater and more varied force requirements, such as aerial drilling [6]. In cases where a full grasp on the target object cannot be achieved, the tilt-rotors can also assist with a forward thrust. This will press the UAV against the target object for a more rigid connection.

We designed a reconfigurable system to minimize the UAV's weight, as it removes the need for an independent gripper and a landing gear. Furthermore, our design improves the UAV's weight distribution. To avoid collision between the propellers and the target object, the gripper must extend beyond the reach of the propellers. This can cause a weight imbalance, limiting stable and efficient flight. Lowering the RLG shifts the center of mass towards the center of the UAV, resulting in improved weight distribution for regular flights.

The RLG has five DoFs (i.e., two joints per finger and one for the reconfiguration). These joints are all coupled via an under-actuated, cable-driven system, which requires only one servo motor for actuation. Such design choice yields a lightweight system and enables the use of a pulley differential to allow for the gripper to conform to the target surface. We place the servo motor near the center of the UAV for improved weight distribution and collision resistance. Figure 3 depicts the system in its key positions. The RLG is passively drawn into the landing gear position in Fig. 3a using elastic cables at the joints. To transition through the remaining positions, the RLG is designed as a series of mechanisms operated by winding in an inelastic cable about the servo drum. The mechanisms are operated sequentially by locking the joints at certain positions via the part geometry.

Manuscript 538 submitted to 2024 IEEE/RSJ International Conference on Intelligent Robots and Systems (IROS). Received February 29, 2024.

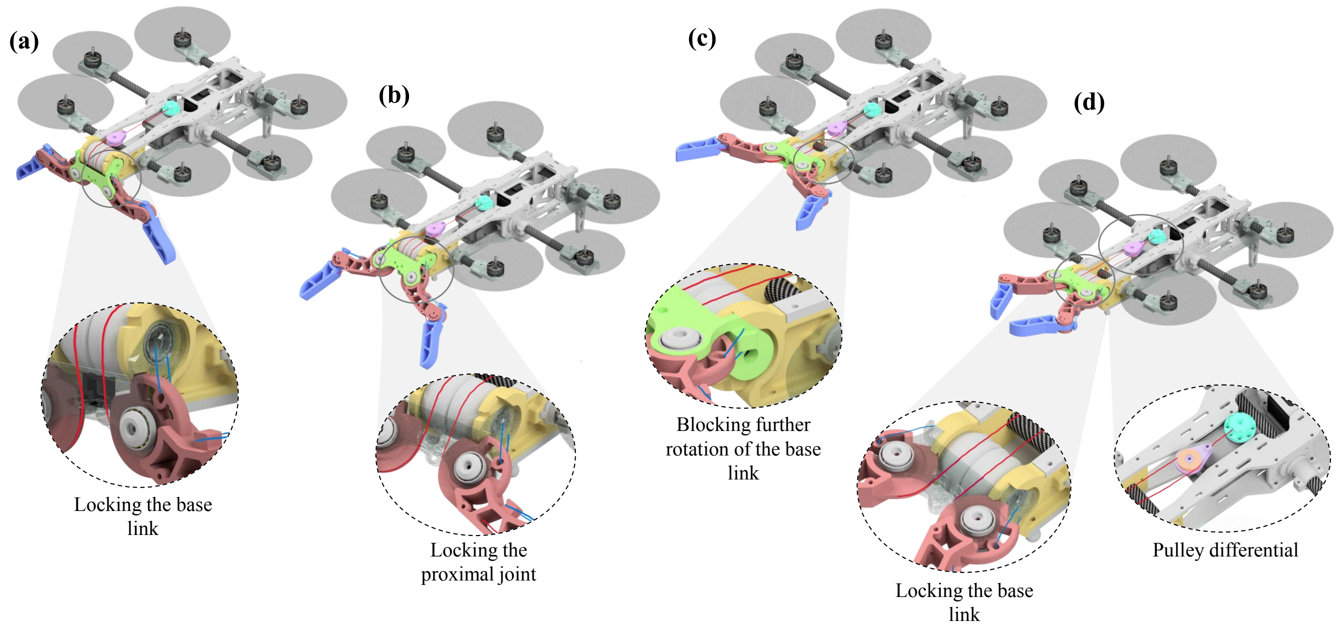

Fig. 3. **The reconfigurable landing gear**, made up of the cable drum (light blue), the pulley differential casing (purple) and the pulley (orange), the RLG mount (yellow), the base link (green), the proximal links (red), and the distal links (dark blue). The inelastic cables (red) and elastic cables (blue) are also depicted. The key positions of the RLG include the **(a)** landing gear position, **(b)** RLG being raised, **(c)** RLG raised and open, and **(d)** closed gripper. Note that the base link (green) is transparent for clarity in certain close-ups.

In the landing gear position shown, locking the base link about the fixed RLG mount is achieved using a disc on the proximal link coupled with a recess in the RLG mount. When grounded, the elastic components, as well as the weight of the UAV, draw the disc into the recess, which acts as a key to prevent the rotation so that the landing gear does not collapse outwards. Once the UAV is in the air, winding in the cable releases this lock, allowing this rotation to occur. As it is being raised, as shown in Fig. 3b, rotation of the proximal link is blocked by the RLG mount, ensuring the gripper cannot close until it is completely raised. Rotation of the distal link in this position is prevented by ensuring the joint has a higher rotational stiffness, such that the force needed to rotate is higher than that needed to raise the RLG. The RLG mount blocks the base link once it reaches the upright position, as shown in Fig. 3c. Closure of the RLG is then shown in Fig. 3d, where the disk on the proximal link can now pass through a slot in the RLG mount. This also provides a lock against the rotation of the base link for improved rigidity. The system acts as an under-actuated gripper in this position, similar to those in [21]. A pulley differential enables the gripper's joints to rotate at differing rates as the cable is wound up, allowing the gripper to conform to the target. Finally, the elastic cables return the RLG to its initial state as the inelastic cable is unwound.

C. Prototype

All structural components were 3D-printed in polylactic acid (PLA) filament, laser-cut from acrylic sheets, or cut from carbon-fiber tubes. We used 1 mm diameter fishing line for the inelastic cable, rubber bands for the elastic components, a thin foam for the contact surface of the

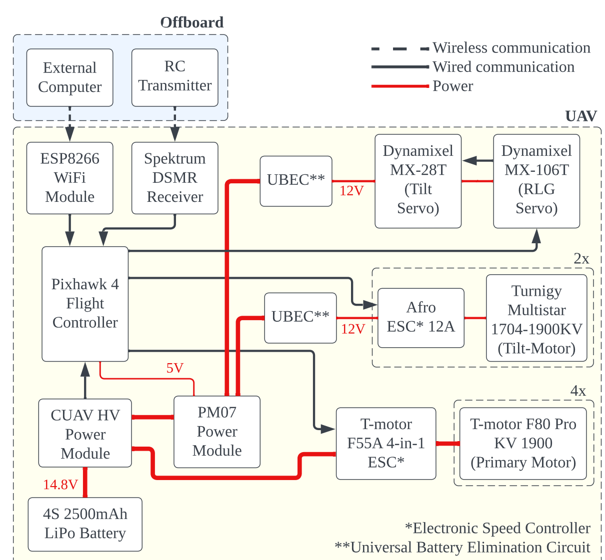

Fig. 4. The electronics architecture implemented for the UAV, including onboard and offboard components.

proximal and distal links of the RLG, and an assortment of steel and nylon fasteners. The electrical components are shown in Fig. 4. The resulting UAV weighs 2.27 kg, with approximately 25% of the mass belonging to the tilt-rotor and RLG components.

III. Control

The following subsections describe the control of the UAV. The control plugins for the tilt-rotors and the RLG were incorporated into the PX4 firmware [22] running on the Pixhawk 4 flight controller.

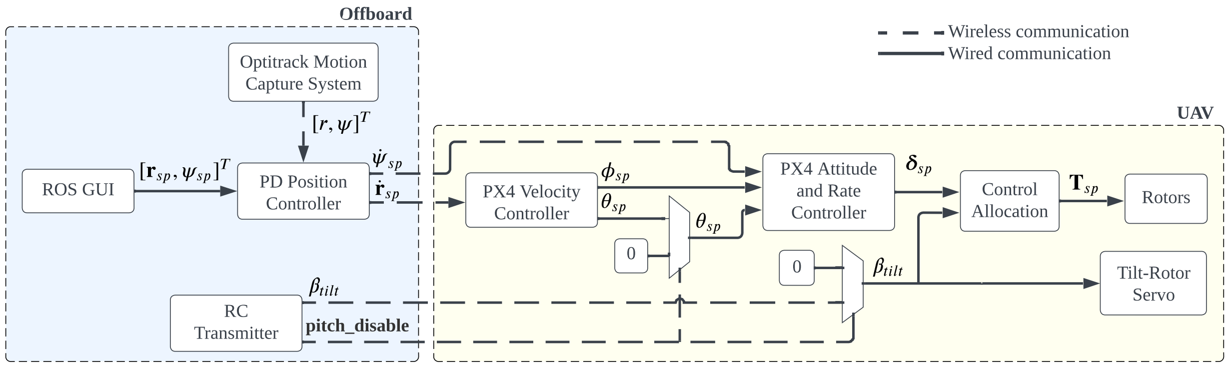

Fig. 5. The control architecture used to operate the UAV. We integrate our system into the existing PX4 control framework [22].

A. Flight Control

In regular flight, the UAV pitches to travel forward and backward. Position control is entirely autonomous using an offboard position controller in the Robot Operating System (ROS) paired with the onboard lower-level PX4 controllers. The tilt-rotors are in the vertical position, thereby providing support for upward thrust. Once pitching is disabled via the RC transmitter, the tilt-rotors start tilting, providing longitudinal force to travel forward and backward. Position in the y and z body frame axes are still controlled autonomously. However, the tilt-angle is directly mapped to the RC transmitter pitch stick, where the maximum point on the pitch stick corresponds to the maximum tilt-angle. This enables an assisted manual flight mode where the UAV operator can maintain some control over the interaction during, for example, inspection or drilling. The speed of the tilt-rotors during this assisted flight mode is adjusted according to the tilt-angle to maintain a constant upward thrust and minimize the disturbance imparted on the system, as per:

$$\omega = \frac{\omega_u}{cos(\beta_{tilt})} \tag{1}$$

where ω is the rotational velocity of the tilt-rotors, ω_u is their rotational velocity when in the upright position, and β_{tilt} is the tilt-angle from the vertical. Note that a limit of ±45° is imposed on the tilt-angle to avoid saturating the tilt-rotors.

The architecture is depicted in Fig. 5. The position vector is $r = [x \;\; y \;\; z]^T$, and the attitude vector is defined as $\Psi = [\phi \;\; \theta \;\; \psi]^T$, which corresponds to roll, pitch, and yaw, respectively. The switch $pitch\_disable$ defines whether pitching or the tilt-rotors are used to generate forward thrust. Finally, $\boldsymbol{\delta}$ contains the torque commands about all three axes and a scalar thrust value: $\boldsymbol{\delta} = [\delta_{\tau_x} \;\; \delta_{\tau_y} \;\; \delta_{\tau_z} \;\; \delta_T]^T$, and $\mathbf{T}$ describes the rotor thrust commands: $\mathbf{T} = [T_1 \;\; T_2 \;\; T_3 \;\; T_4 \;\; T_5 \;\; T_6]^T$. The input to the PX4 attitude and rate controller is a quaternion setpoint; however, Euler angles are shown for simplicity. We obtain position feedback using an external motion capture (MoCap) system.

B. Articulated Landing Gear Control

The articulated landing gear is controlled by defining three positions of the Dynamixel MX-106T servo motor, which operates in continuous mode. Each position corresponds to one of the following three states: landing gear position (Fig. 3a), gripper raised and open (Fig. 3c), and gripper raised and closed[1] (Fig. 3d). The current state is selected during flight using the RC transmitter.

IV. Testing

We conducted several real-world experiments to assess the UAV's performance, including free-flight and interaction tests. These are outlined in the following subsections.

A. Independent forward thrust

We begin by verifying the UAV's ability to generate an independent forward thrust without pitching. This ability will enable more controlled movement when approaching a target for interaction and will support the RLG for improved grasping. We conduct two flights: a typical under-actuated flight where pitching is required to move forward and a flight where only thrust vectoring by tilt-rotors is used for moving forward. In both flights, the UAV navigates 1 m forward from its initial position. The forward speed is similar across the two tests, albeit slightly varied due to the assisted manual flight mode used during the tilt-rotor flight. The results are shown in Fig. 6. As expected, when transitioning from under-actuated flight to tilt-rotor flight, the UAV could travel forward with a greatly reduced change in pitch angle.

B. Interaction

Next, we test the UAV's ability to achieve high position accuracy during physical interaction. We perform an ablation study to identify the contributions of the tilt-rotors and the RLG to the UAV's performance. This includes running the following tests, referred to as Test 1 (T1), Test 2 (T2), and Test 3 (T3):

- T1: Traditional station-keeping next to the target object without tilt-rotors or RLG, as a baseline.
- T2: Station-keeping while grasping onto the target object without tilting the rotors.
- T3: Station-keeping while grasping onto the target object with support from the tilt-rotors.

[1]Note that this final position must be tuned for current testing purposes to fit the size of the tree being grasped.

Manuscript 538 submitted to 2024 IEEE/RSJ International Conference on Intelligent Robots and Systems (IROS). Received February 29, 2024.

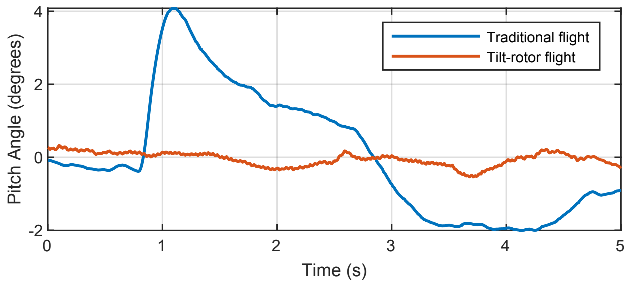

Fig. 6. Orientation data during flight from $x = 0$ to $x = 1\,\mathrm{m}$ to verify the UAV's ability to generate an independent forward thrust.

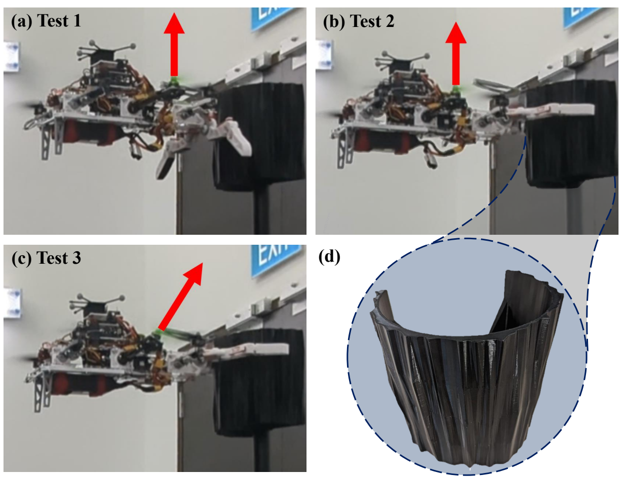

Fig. 7. The tests for assessing the performance of the RLG and the tilt-rotors. **(a)** T1 involves traditional station-keeping. **(b)** T2 adds the use of the RLG, while **(c)** T3 further adds the use of the tilt-rotors. The red arrows depict the direction of tilt-rotor thrust. **(d)** The 3D-printed target object used for testing has a rough outer surface designed to mimic tree bark.

The three tests are depicted in Fig. 7. The target object has a diameter of approximately 210 mm, which is intentionally larger than what the RLG can fully grasp. This allows us to validate the performance of the tilt-rotors and RLG when working cooperatively. The target object is 3D-printed from PLA, with a textured outer surface to mimic tree bark.

The UAV's deviation from the initial position (given as the Euclidean norm) and from the initial heading in each test is shown in Fig. 8. It is clear from T1 that the UAV's free-flight station-keeping performance is limited. During the 10-second period of interaction, the UAV deviated from its initial position by up to 51 mm, and from its initial heading by 8°. T2 showed initial improvement, demonstrating the potential for the gripper to improve precision. However, pitching of the UAV loosened the RLG's grasp on the target object over time, causing the UAV to drift into traditional station-keeping after approximately 5 seconds. This resulted in no overall improvement compared to T1. Finally, in T3, we disabled pitch and provided a constant forward force using the tilt-rotors to assist the RLG in maintaining contact with the target. This resulted in significantly more stable contact. The UAV only deviated from its initial position by at most 7mm and from its initial heading by approximately 1°. Compared to T1, this is a reduction in maximum deviation in position and heading of 86% and 88%, respectively.

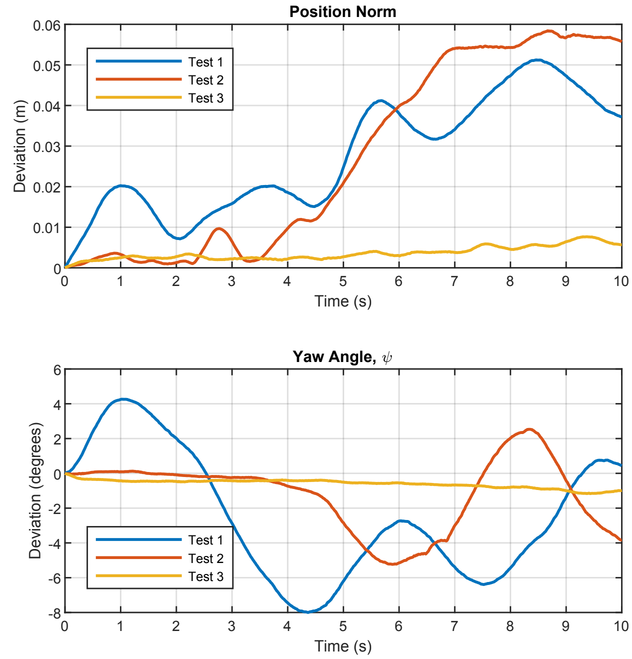

Fig. 8. Deviation from the initial position and heading during 10 seconds of interaction. We report the ground truth data from the MoCap system.

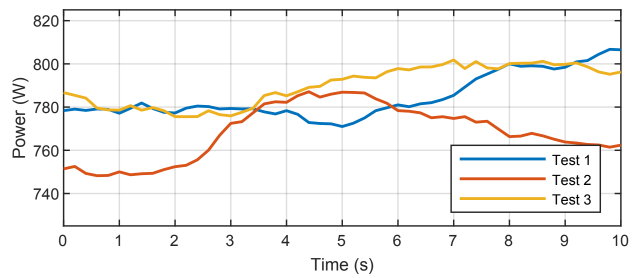

Fig. 9. UAV power consumption during testing, which shows minimal loss in efficiency caused by the tilt-rotors and RLG.

We also recorded the power consumption of the UAV during each test using the CUAV HV power module, as shown in Fig. 9. During T1, the UAV had an average power consumption of approximately 785 W. We note that during T1, which acts as our baseline, the UAV carries the weight of the tilt-rotor and RLG components without using them. Hence, this power consumption value is likely inflated. During the start of T2, when the RLG was grasping the target object, this appeared to alleviate some of the effort required by the rotors, reducing the average power consumption of the UAV to approximately 770 W. Finally, the addition of the tilt-rotors offset that reduction in power consumption, raising the average to about 790 W. Overall, we achieved significant performance improvements from T1 to T3 at the cost of a less than 1% increase in average power consumption.

V. Limitations

Despite demonstrating promising performance gains, there are limitations to the current system. Firstly, given that the RLG positions are hard-coded, we are not effectively using the RLG's ability to conform to the target object's shape. In future work, we will use feedback from the servo motor (e.g., current drawn) to define a point for the gripper to stop closing. While this should allow for an improved grasp, it may also affect the UAV's power consumption.

There are also limitations of the UAV's flight control. Firstly, MoCap is used for state estimation during our experiments, which does not translate to real-world environments. Hence, alternative methods, such as visual servoing for approaching the target, will be explored. Furthermore, during interaction, the UAV maintains its position where the grasp is initiated. This position may not be aligned with the current position setpoint due to the UAV's limited free-flight position control performance. Since the setpoint is static, the controller will attempt to oppose the support from the gripper. Visual servoing would rectify this problem to some extent by eliminating the use of a global setpoint. However, we will also look into implementing a more interaction-friendly control scheme, such as admittance control [23].

VI. Conclusion

In this work, we presented a UAV design with tilt-rotors and a reconfigurable landing gear. These mechanisms enable the UAV to obtain support from a target object during physical interaction applications and improve the control accuracy. When both mechanisms are activated, the position and heading control accuracy of the UAV is improved by 86% and 88%, respectively, while flying against a vertical, cylindrical target object with a rough surface. Our future work will include assessing the size of the independent forces and torques the UAV can generate during the interaction. We will then apply our system to real-world, high-precision, contact-based applications. We will also explore greater autonomy of the UAV during interaction, which includes adding feedback to the RLG's control system and implementing more interaction-friendly flight control.

ACKNOWLEDGMENT

The authors would like to thank Mohammad Asif for his help in running the experiments.

References

[1] Teodor Tomic, Korbinian Schmid, Philipp Lutz, Andreas Domel, Michael Kassecker, Elmar Mair, Iris Lynne Grixa, Felix Ruess, Michael Suppa, and Darius Burschka. Toward a fully autonomous uav: Research platform for indoor and outdoor urban search and rescue. *IEEE robotics & automation magazine*, 19(3):46–56, 2012.

[2] Jan C van Gemert, Camiel R Verschoor, Pascal Mettes, Kitso Epema, Lian Pin Koh, and Serge Wich. Nature conservation drones for automatic localization and counting of animals. In *Computer Vision-ECCV 2014 Workshops: Zurich, Switzerland, September 6-7 and 12, 2014, Proceedings, Part I 13*, pages 255–270. Springer, 2015.

[3] Roman Dautzenberg, Timo Küster, Timon Mathis, Yann Roth, Curdin Steinauer, Gabriel Käppeli, Julian Santen, Alina Arranhado, Friederike Biffar, Till Kötter, et al. A perching and tilting aerial robot for precise and versatile power tool work on vertical walls. In *2023 IEEE/RSJ International Conference on Intelligent Robots and Systems (IROS)*, pages 1094–1101. IEEE, 2023.

[4] Lei Yang, Junfeng Fan, Yanhong Liu, En Li, Jinzhu Peng, and Zize Liang. A review on state-of-the-art power line inspection techniques. *IEEE Transactions on Instrumentation and Measurement*, 69(12):9350–9365, 2020.

[5] Christian Geckeler and Stefano Mintchev. Bistable helical origami gripper for sensor placement on branches. *Advanced Intelligent Systems*, 4(10):2200087, 2022.

[6] Caiwu Ding, Lu Lu, Cong Wang, and Caiwen Ding. Design, sensing, and control of a novel uav platform for aerial drilling and screwing. *IEEE Robotics and Automation Letters*, 6(2):3176–3183, 2021.

[7] Micha Schuster, David Bernstein, Paul Reck, Salua Hamaza, and Michael Beitelschmidt. Automated aerial screwing with a fully actuated aerial manipulator. In *2022 IEEE/RSJ International Conference on Intelligent Robots and Systems (IROS)*, pages 3340–3347. IEEE, 2022.

[8] Pedro Henrique Mendes Souza and Karl Stol. Constrained dynamics of an aerial manipulator interacting with flexible cantilever beams. *IEEE/ASME Transactions on Mechatronics*, 28(2):967–975, 2022.

[9] Jasper LJ Scholten, Matteo Fumagalli, Stefano Stramigioli, and Raffaella Carloni. Interaction control of an uav endowed with a manipulator. In *2013 IEEE International Conference on Robotics and Automation*, pages 4910–4915. IEEE, 2013.

[10] T Bartelds, Alex Capra, Salua Hamaza, Stefano Stramigioli, and Matteo Fumagalli. Compliant aerial manipulators: Toward a new generation of aerial robotic workers. *IEEE Robotics and Automation Letters*, 1(1):477–483, 2016.

[11] Karen Bodie, Maximilian Brunner, Michael Pantic, Stefan Walser, Patrick Pfändler, Ueli Angst, Roland Siegwart, and Juan Nieto. Active interaction force control for contact-based inspection with a fully actuated aerial vehicle. *IEEE Transactions on Robotics*, 37(3):709–722, 2020.

[12] Takamasa Kominami, Zou Liang, Ricardo Rosales Martinez, Hannibal Paul, and Kazuhiro Shimonomura. Physical contact with wall using a multirotor uav equipped with add-on thruster for inspection work. In *2023 IEEE/RSJ International Conference on Intelligent Robots and Systems (IROS)*, pages 6955–6961. IEEE, 2023.

[13] William RT Roderick, Mark R Cutkosky, and David Lentink. Bird-inspired dynamic grasping and perching in arboreal environments. *Science Robotics*, 6(61):eabj7562, 2021.

[14] Andrew McLaren, Zak Fitzgerald, Geng Gao, and Minas Liarokapis. A passive closing, tendon driven, adaptive robot hand for ultra-fast, aerial grasping and perching. In *2019 IEEE/RSJ International Conference on Intelligent Robots and Systems (IROS)*, pages 5602–5607. IEEE, 2019.

[15] HaoTse Hsiao, Jiefeng Sun, Haijie Zhang, and Jianguo Zhao. A mechanically intelligent and passive gripper for aerial perching and grasping. *IEEE/ASME Transactions on Mechatronics*, 27(6):5243–5253, 2022.

[16] Weijia Tao, Karishma Patnaik, Fuchen Chen, Yogesh Kumar, and Wenlong Zhang. Design, characterization and control of a whole-body grasping and perching (whopper) drone. In *2023 IEEE/RSJ International Conference on Intelligent Robots and Systems (IROS)*, pages 1–7. IEEE, 2023.

[17] Jim David Ang, Lester Librado, Carl John Salaan, Jonathan Maglasang, Kristine Sanchez, and Marcelo Ang. Drone with pneumatic-tethered suction-based perching mechanism for high payload application. In *2022 IEEE/RSJ International Conference on Intelligent Robots and Systems (IROS)*, pages 12154–12161. IEEE, 2022.

[18] Han W Wopereis, TD Van Der Molen, TH Post, Stefano Stramigioli, and Matteo Fumagalli. Mechanism for perching on smooth surfaces using aerial impacts. In *2016 IEEE international symposium on safety, security, and rescue robotics (SSRR)*, pages 154–159. IEEE, 2016.

[19] Jeffrey Mao, Stephen Nogar, Christopher M Kroninger, and Giuseppe Loianno. Robust active visual perching with quadrotors on inclined surfaces. *IEEE Transactions on Robotics*, 2023.

[20] Liming Zheng and Salua Hamaza. Albero: Agile landing on branches for environmental robotics operations. *IEEE Robotics and Automation Letters*, 2024.

[21] Raymond Ma and Aaron Dollar. Yale openhand project: Optimizing open-source hand designs for ease of fabrication and adoption. *IEEE Robotics & Automation Magazine*, 24(1):32–40, 2017.

[22] Lorenz Meier, Dominik Honegger, and Marc Pollefeys. Px4: A node-based multithreaded open source robotics framework for deeply embedded platforms. In *2015 IEEE international conference on robotics and automation (ICRA)*, pages 6235–6240. IEEE, 2015.

[23] Federico Augugliaro and Raffaello D'Andrea. Admittance control for physical human-quadrocopter interaction. In *2013 European Control Conference (ECC)*, pages 1805–1810. IEEE, 2013.